

# Nickel aluminide (Ni<sub>3</sub>Al) fabricated by reactive infiltration

YUYONG CHEN, D. D. L. CHUNG

*Composite Materials Research Laboratory, State University of New York at Buffalo, Buffalo, NY 14260-4400, USA*

Nickel aluminide Ni<sub>3</sub>Al in the single phase form, with grain size  $\sim 10\ \mu\text{m}$ , porosity  $\sim 5\%$ , tensile strength 425 MPa, modulus 92 GPa and ductility 9.5% at room temperature, was fabricated by reactive infiltration at 800 °C of liquid aluminium into a porous preform containing 78 vol% nickel and made by sintering 3–7  $\mu\text{m}$  size nickel particles. Without sintering, the preform contained 58 vol% nickel and reactive infiltration resulted in an aluminium-matrix NiAl<sub>3</sub> particle ( $\sim 50\ \mu\text{m}$  size) composite and extensive growth of Ni–Al needles from the preform to the excess liquid aluminium around the preform.

## 1. Introduction

Intermetallics are well-known for their combination of high strength and high temperature resistance, so they are useful for turbine components, aerospace structures and other high temperature applications. However, the fabrication of intermetallics is costly, thus making intermetallics not widely available.

The fabrication of an intermetallic from its constituent elements (e.g., Ni<sub>3</sub>Al from Ni and Al) has been carried out by arc melting, combustion synthesis [1], reactive sintering [2] and reactive infiltration [3–6]. Reactive sintering refers to the sintering of a mixture of the constituent metal powders to form the intermetallic, whereas reactive infiltration refers to the liquid phase infiltration of the constituent metal with the lower melting point into a porous preform made of the other constituent metal, thereby forming the intermetallic. Advantages of reactive infiltration include the following: (a) faster than reactive sintering, (b) lower temperature than arc melting or combustion synthesis, (c) suitable for composites, and (d) near net-shape.

Infiltration of a liquid metal into a porous preform can be carried out by pressure casting (i.e. applying isostatic pressure on the liquid metal to force the infiltration to take place) and squeeze casting (i.e. applying a ram to push on the liquid metal in order to force the infiltration to take place). The pressure serves to hasten the infiltration and enhance the wetting of the preform by the liquid metal. Squeeze casting tends to have a shorter turn-around time than pressure casting, but its association with a higher rate of pressure increase tends to cause preform compression (thus not near-net-shape) or even preform cracking.

Previous work on nickel aluminide fabricated by reactive infiltration involved pressure casting [3–5] and squeeze casting [6]. By using pressure casting, Dunand *et al.* [3] fabricated NiAl as a single phase,

but not Ni<sub>3</sub>Al in a single phase. Chen *et al.* [4, 5] made neither NiAl nor Ni<sub>3</sub>Al in single phase form using pressure casting. Suganuma [6] made Ni<sub>3</sub>Al in a single phase by using Ni<sub>3</sub>Al, but did not make NiAl in a single phase. This means that pressure casting has not been previously used to make Ni<sub>3</sub>Al in a single phase, although squeeze casting has. Because the difficulty of infiltration increases with increasing solid (nickel) content in the preform (i.e. decreasing porosity in the preform), the making of Ni<sub>3</sub>Al by reactive infiltration is more challenging than that of NiAl. Therefore, an objective of this work was to use pressure casting to make single phase Ni<sub>3</sub>Al.

Little attention has been given by previous workers to the mechanical properties of nickel aluminide fabricated by reactive infiltration. Neither Chen *et al.* [4, 5] nor Dunand *et al.* [3] reported any tensile properties. Suganuma [6] reported that their Ni<sub>3</sub>Al had a tensile strength of 400 MPa and a tensile ductility described as “little elongation” or “brittle”. A second objective of this work was to determine the tensile strength and ductility of Ni<sub>3</sub>Al fabricated by pressure infiltration. A third objective was to obtain tensile properties that were better (especially in ductility) than those previously reported.

## 2. Experimental details

### 2.1. Ni<sub>3</sub>Al fabrication

The nickel particles were 3–7  $\mu\text{m}$  in size, as provided by INCO as Type 123. The nickel particle preform (36 mm diameter, 15 mm height) was formed by wet forming an Ni–H<sub>2</sub>O slurry containing a small amount of an acid phosphate binder [7]. The wet forming was performed by cold pressing at 5 MPa. After that, the preform was removed from the mould and dried at 200 °C for 24 h. After drying, the preform was heated in air at 400 °C for 4 h. It contained 58 vol% Ni. The binder (aluminium metaphosphate) constituted

~ 0.1 wt % of the preform. Subsequently, the preform was sintered at 1050 °C in vacuum ( $10^{-2}$  torr) for 1 h. After sintering, the preform contained 78 vol % Ni.

The aluminium used was pure aluminium (no. 170.1), the melting point of which was 660 °C. The composite was made by vacuum infiltration of the liquid aluminium under an argon pressure of 41 MPa (6000 p.s.i.) and at an infiltration temperature of 800 °C. A steel mould was used. The process is similar to that of [8]. After infiltration, no heat treatment was conducted.

## 2.2. Ni<sub>3</sub>Al characterization

X-ray diffraction was conducted using a diffractometer and CuK<sub>α</sub> radiation. Fig. 1 shows the X-ray diffraction pattern. The only diffraction peaks observed were those of Ni<sub>3</sub>Al, indicating that the material was a single phase. No nickel or aluminium remained.

Microstructural characterization of the composite included optical metallography and scanning electron microscopy (SEM). Metallographic samples were sectioned with a low-speed diamond saw, ground and then polished with a diamond paste. Etching was conducted at room temperature by immersion in a solution containing 50 ml HCl, 50 ml H<sub>2</sub>O and 10 g CuSO<sub>4</sub>. Light etching and deep etching differed only in the etching time, which was 3–5 min for light etching and 30 min for deep etching. Fig. 2 shows the optical micrographs obtained after light etching. It revealed the grain boundaries and some porosity (about 5%) along the grain boundaries. It also showed

that the grain size was about 10 μm. Fig. 3 shows the SEM photographs obtained after light etching; grains (~ 10 μm size) and pores were similarly observed.

Room temperature tensile properties were obtained in air on three dog-bone-shaped specimens using a Sintech 2/D screw-type mechanical testing system and strain gauges for measuring the modulus. The ductility was obtained by measuring the change in distance between two lines (~ 8 mm apart initially) drawn perpendicular to the stress axis. The strain rate was  $4 \times 10^{-5} \text{ s}^{-1}$ . The tensile strength was 425 (± 4) MPa; the tensile modulus was 92 (± 3) GPa; the tensile ductility was 9.5 (± 0.5)%.

## 2.3. Aluminium-matrix NiAl<sub>3</sub> composite fabrication and characterization

Using the same procedure as described in Section 2.1, except that the step of preform sintering was skipped, an aluminium-matrix composite containing > 60 vol % NiAl<sub>3</sub> (~ 50 μm particles) was obtained. This is a consequence of the low nickel volume fraction (58%) in the preform, in contrast to the nickel volume fraction of 78% that resulted in Ni<sub>3</sub>Al. X-ray diffraction (Fig. 4) shows the presence of two phases, namely Al and NiAl<sub>3</sub>. No Ni<sub>3</sub>Al was observed. For the microstructure of this composite, see Section 2.4.

## 2.4. Interface between the product and the excess aluminium cast around it

The interface between the Al/NiAl<sub>3</sub> composite and the excess aluminium cast around it is shown in Fig. 5,

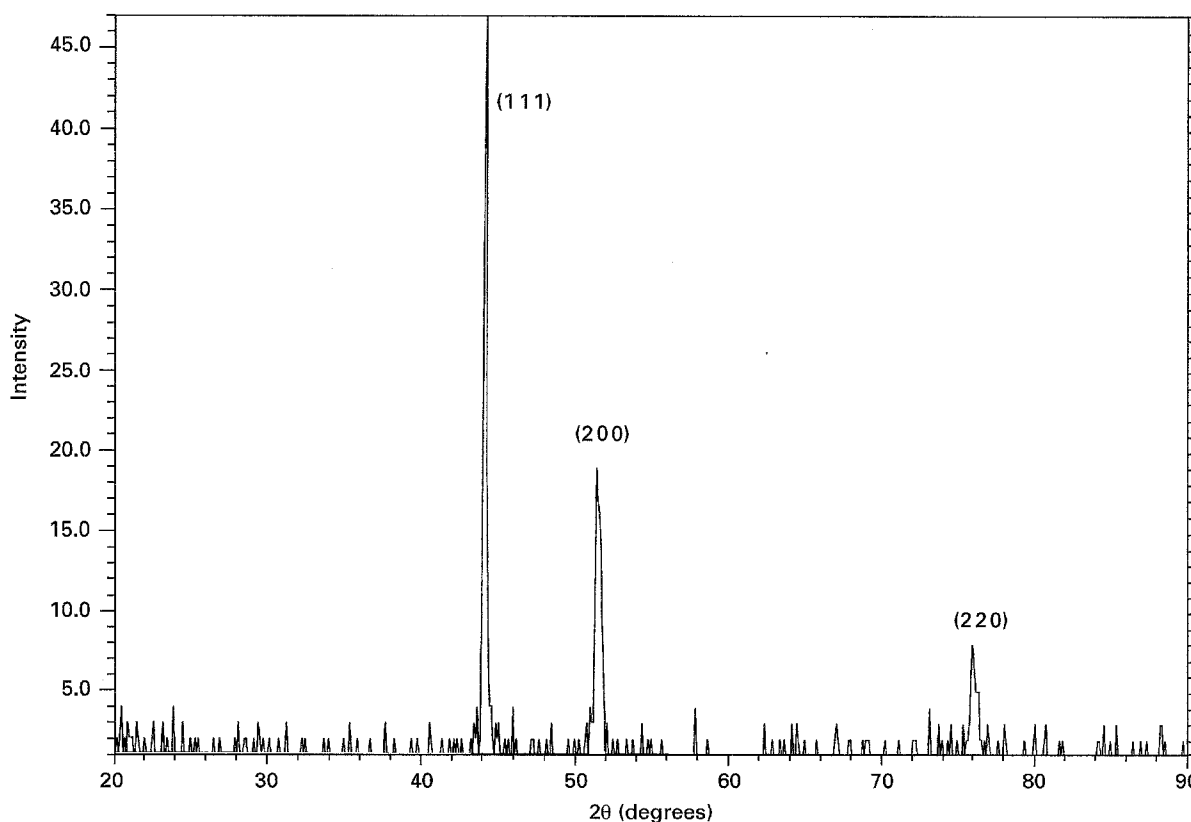


Figure 1 X-ray diffraction pattern of Ni<sub>3</sub>Al obtained in this work.

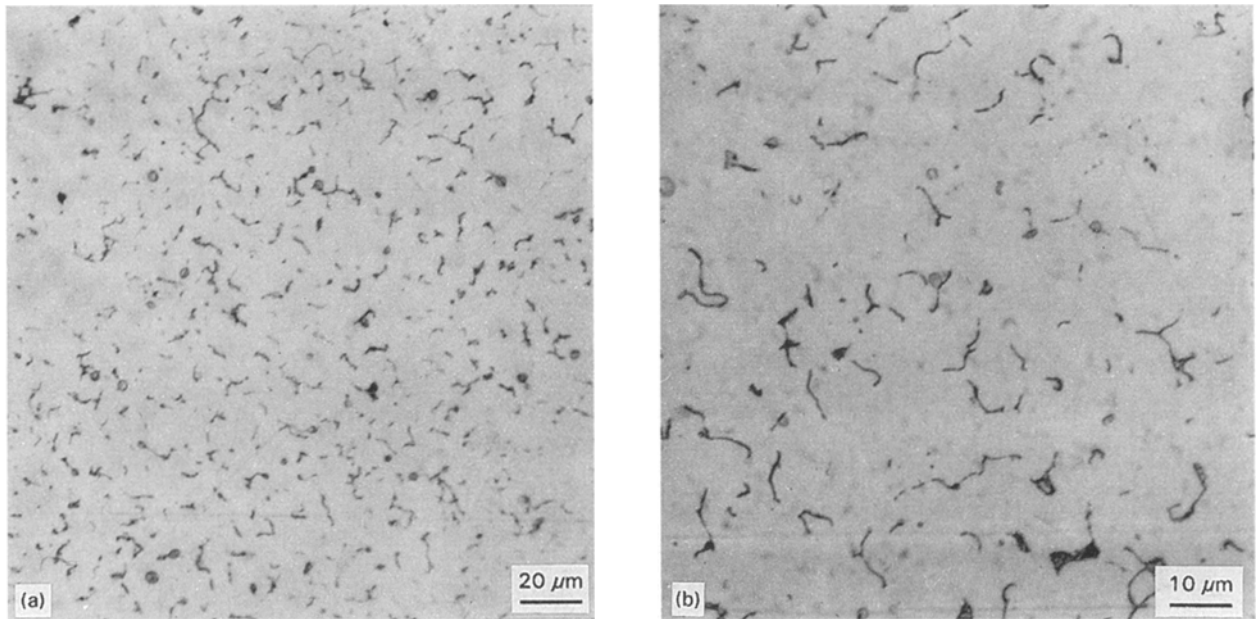


Figure 2 Optical micrographs obtained after light etching of the  $\text{Ni}_3\text{Al}$  of this work.

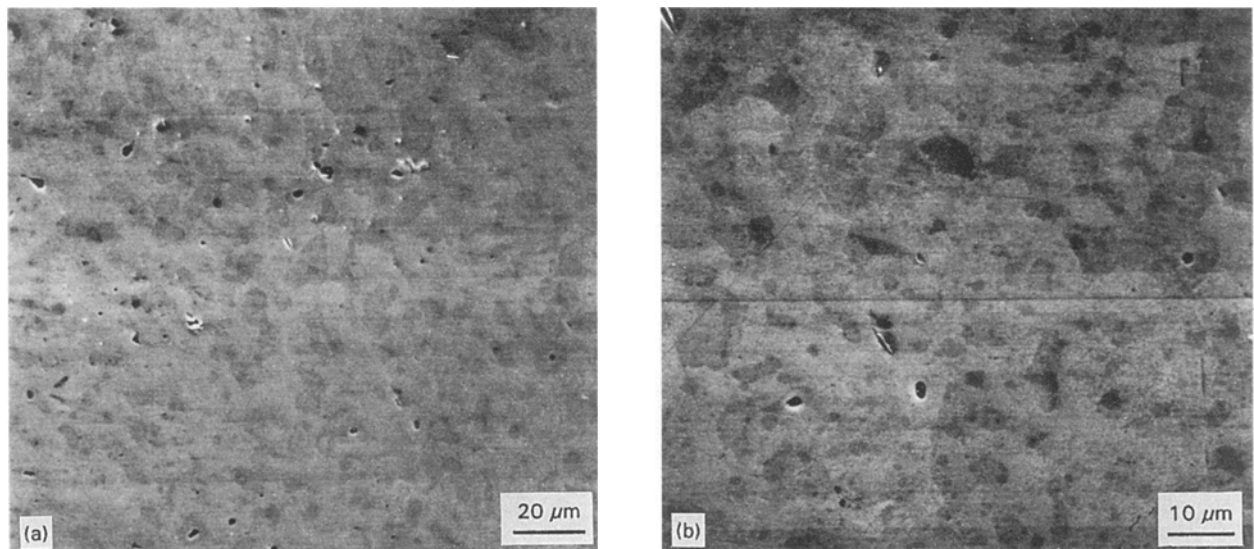


Figure 3 SEM photographs obtained after light etching of the  $\text{Ni}_3\text{Al}$  of this work.

as revealed by SEM. Fig. 5a was obtained after light etching; its upper 40% was the excess aluminium while its lower 60% was the composite. Fig. 5b was obtained after deep etching; its upper 2/3 was the excess aluminium while its lower 1/3 was the composite. Both Fig. 5a and b show the growth of needle-shaped  $\text{NiAl}_3$  grains from the composite toward the excess aluminium. Fig. 6 shows high magnification views after deep etching of the needle-shaped  $\text{NiAl}_3$  grains in the excess aluminium region (Fig. 6a) and the equiaxed  $\text{NiAl}_3$  grains of size  $\sim 50 \mu\text{m}$  in the composite (Fig. 6b). As a result of the growth of  $\text{NiAl}_3$  toward the excess aluminium, the preform was partly consumed, thus resulting in a composite of height much less than the height of the original preform, as illustrated in Fig. 7a.

Much less Ni–Al needle growth was observed at the interface between the  $\text{Ni}_3\text{Al}$  and the excess aluminium

cast around it, as illustrated in Fig. 7b. Fig. 8 (obtained by SEM after light etching) shows the excess aluminium region only. The excess aluminium region contained needle-shaped grains of primary Ni–Al, together with a lamellar Ni–Al eutectic microconstituent. Due to the near absence of Ni–Al needle growth across the interface, the height of the product was essentially the same as the height of the original preform, as illustrated in Fig. 7b.

As illustrated in Fig. 7, the fabrication of Al/ $\text{NiAl}_3$  was not near net-shape, whereas that of  $\text{Ni}_3\text{Al}$  was.

### 3. Discussion

A simple calculation shows that the nickel volume fraction in a nickel–aluminium two-phase mixture for forming  $\text{Ni}_3\text{Al}$  in a single phase form is 66%. However, with 78 vol % nickel in the preform, we formed

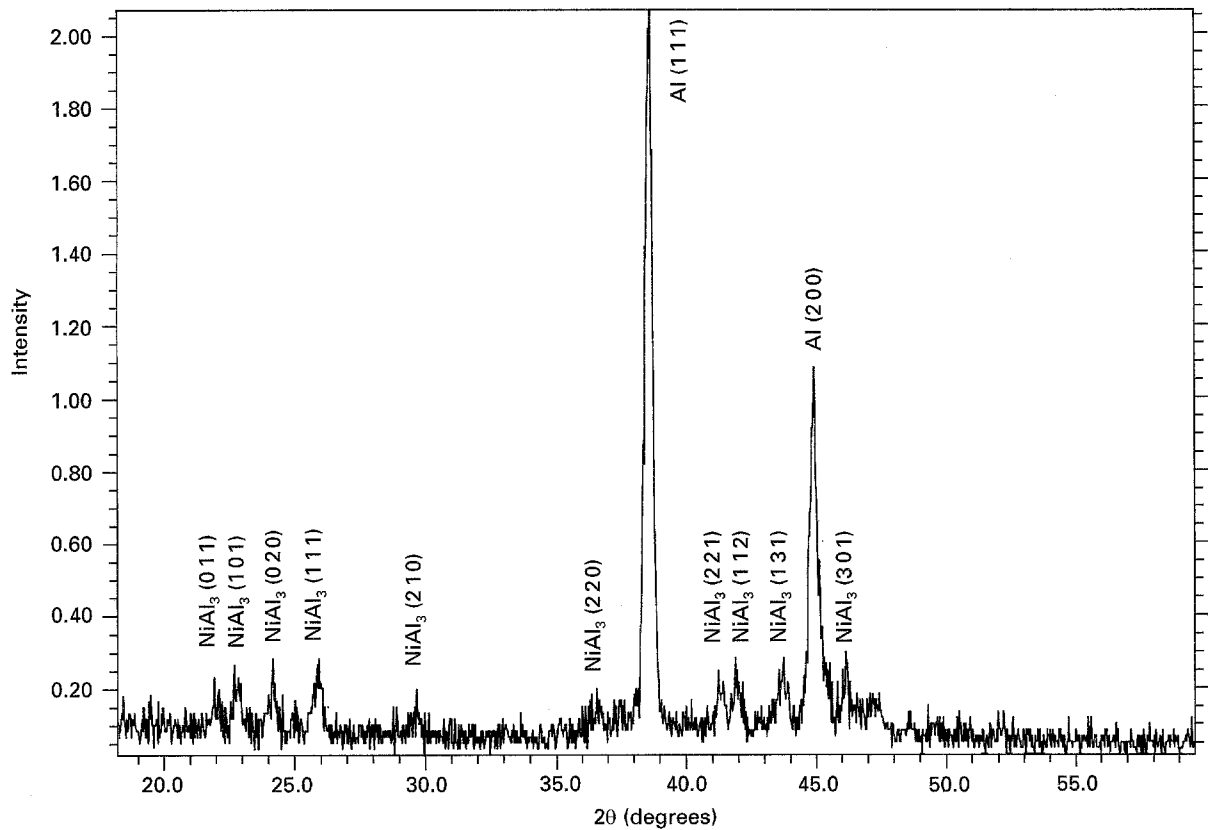


Figure 4 X-ray diffraction pattern of Al/NiAl<sub>3</sub> obtained in this work.

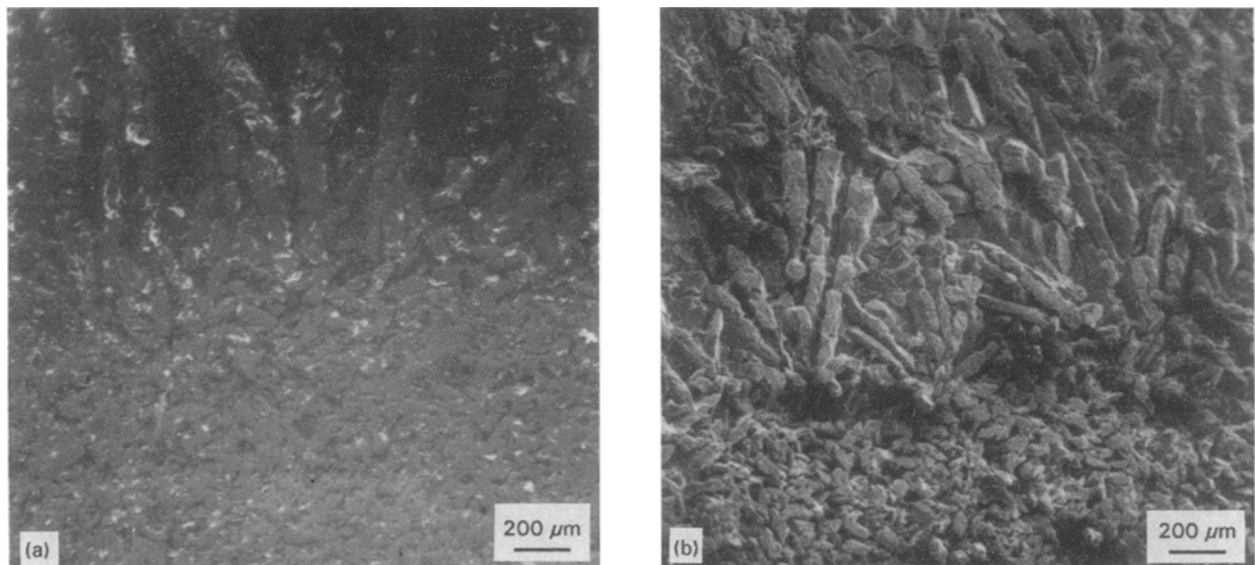


Figure 5 SEM photographs obtained after (a) light etching and (b) deep etching of the interface between the Al/NiAl<sub>3</sub> composite and the excess aluminium cast around the composite.

Ni<sub>3</sub>Al in a single phase form. This is attributed partly to the Ni–Al needles that grew from the nickel preform toward the excess liquid aluminium during reactive infiltration and partly to the composition variability within the Ni<sub>3</sub>Al single-phase field in the Ni–Al binary phase diagram.

When the preform contained only 58 vol % nickel, the Ni–Al needle growth was much more extensive (so that the process was not near net-shape) and an Al/NiAl<sub>3</sub> composite was formed instead of Ni<sub>3</sub>Al. The much more extensive Ni–Al growth when the preform

contained less nickel is due to the larger channels of liquid aluminium in the preform during reactive infiltration and the consequent greater ease of nickel out-diffusion toward the excess liquid aluminium around the preform. As a result of the extensive Ni–Al needle growth (i.e. the loss of Ni), Al/NiAl<sub>3</sub> rather than NiAl, Al/NiAl or Al/Ni<sub>3</sub>Al was formed.

A comparison between this work and [6] is shown in Table I. The Ni<sub>3</sub>Al of this work exhibits higher ductility than that of [6], though the strength is similar. The difference in ductility is probably due to

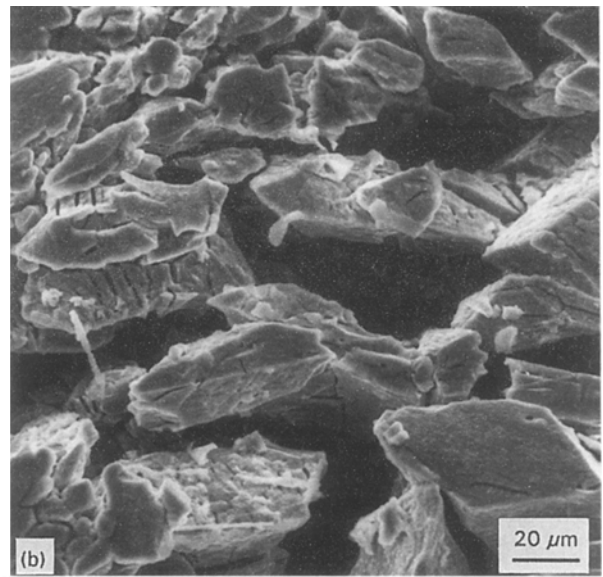
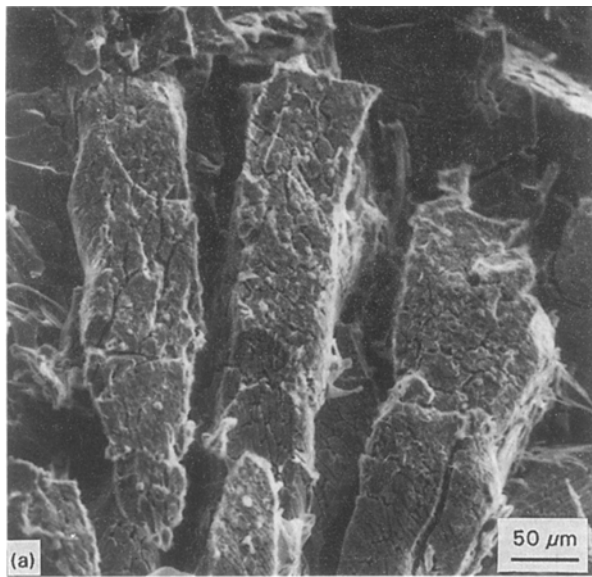


Figure 6 SEM photographs obtained after deep etching of (a) the needle-shaped  $\text{NiAl}_3$  grains in the excess aluminium region, and (b) the equiaxed  $\text{NiAl}_3$  grains in the  $\text{Al}/\text{NiAl}_3$  composite.

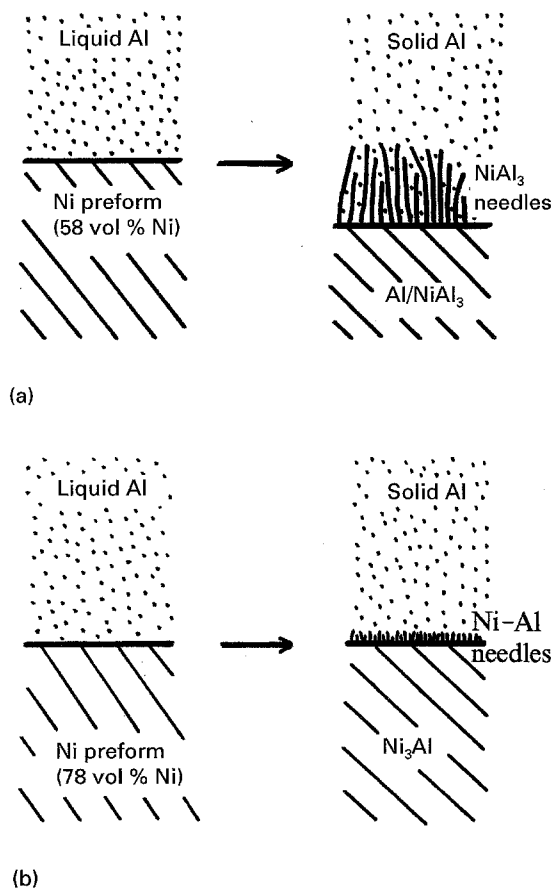


Figure 7 Schematic illustration of the interface between the product and the excess aluminium. (a) The preform contained 58 vol % Ni and the process was not near net-shape. (b) The preform contained 78 vol % Ni and the process was near net-shape.

(i) the much smaller nickel particle size used in this work, (ii) the use of an Al ingot instead of Al powder in this work and the resulting smaller amount of  $\text{Al}_2\text{O}_3$  contamination, and (iii) that the liquid aluminium infiltration was conducted after evacuation (rather than just in air) in this work.

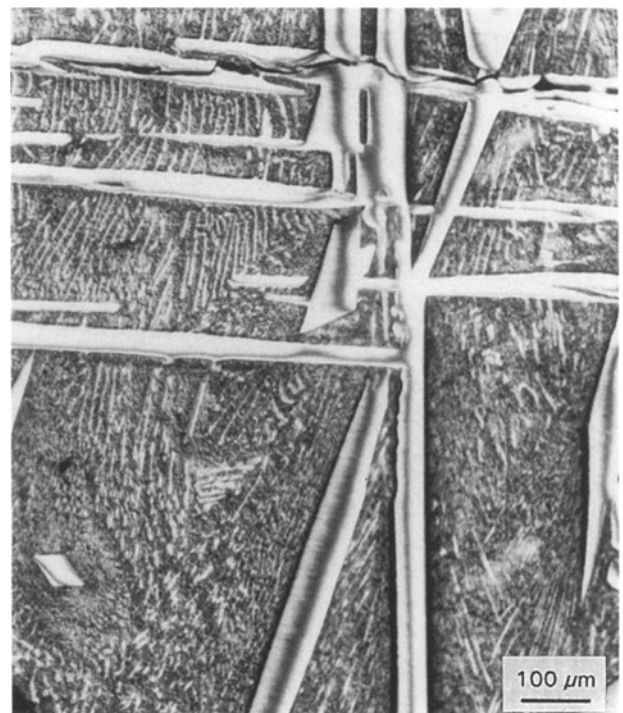


Figure 8 SEM photograph obtained after light etching of the excess aluminium region around  $\text{Ni}_3\text{Al}$ .

TABLE I Comparison between this work and [6]

	This work	[6]
Casting method	Pressure	Squeeze
Preform sintering	1050 °C	1200 °C
Ni in preform	78 vol %	65 vol %
Preform temperature <sup>a</sup>	800 °C	550 °C
Mould temperature <sup>a</sup>	800 °C	450 °C
Pressure <sup>a</sup>	41 MPa	50 MPa
Ni particle size	3–7 μm	< 44 μm
Phase formed	$\text{Ni}_3\text{Al}$	$\text{Ni}_3\text{Al}$
Tensile strength <sup>c</sup>	425 MPa	400 MPa <sup>b</sup>
Tensile ductility <sup>c</sup>	9.5%	Little elongation <sup>b</sup>

<sup>a</sup> During infiltration.

<sup>b</sup> Strain rate unknown.

<sup>c</sup> Room temperature, in air.

#### 4. Conclusion

Nickel aluminide  $\text{Ni}_3\text{Al}$  in single phase form, with grain size  $\sim 10\ \mu\text{m}$  and porosity  $\sim 5\%$ , was fabricated by reactive infiltration of liquid aluminium into a nickel particle preform containing 78 vol % nickel and 12 vol % porosity. The nickel preform was prepared by wet forming and then sintering. (Prior to sintering, the preform contained 58 vol % nickel.) The preform was made from nickel particles of size 3–7  $\mu\text{m}$ . The  $\text{Ni}_3\text{Al}$  obtained exhibited tensile strength 425 MPa, modulus 92 GPa and ductility 9.5% at room temperature. Without sintering the preform, infiltration resulted in an aluminium-matrix  $\text{NiAl}_3$  ( $\sim 50\ \mu\text{m}$ ) particle composite and extensive growth of  $\text{NiAl}_3$  needles from the preform to the excess liquid aluminium around the preform.

#### References

1. J. P. LEBRAT, A. VARMA and P. J. MCGINN, *J. Mater. Res.* **9** (1994) 1184.
2. N. S. STOLOFF and D. E. ALMAN, *Mater. Sci. Eng.* **A144** (1991) 51.
3. D. C. DUNAND, J. L. SOMMER and A. MORTENSEN, *Metall. Trans. A* **24A** (1993) 2161.
4. H. CHEN, M. KAYA and R. W. SMITH, *Mater. Lett.* **13** (1992) 180.
5. *Idem*, in Adv. Prod. Fabr. Light Met. Met. Matrix Compos., Proceedings of the International Symposium, edited by M. M. Avedesian, L. J. Larouche and J. Masounave (Canadian Institute of Mining, Metallurgical and Petroleum Engineers, Montreal, Canada, 1992) pp. 549–558.
6. K. SUGANUMA, *Mater. Lett.* **16** (1993) 22.
7. JENG-MAW CHIOU and D. D. L. CHUNG, *J. Mater. Sci.* **28** (1993) 1471.
8. JINGYU YANG and D. D. L. CHUNG, *ibid.* **24** (1989) 3605.

*Received 12 January*

*and accepted 4 October 1995*